anyMOD – A graph-based framework for energy system modelling with high levels of renewables and sector integration

Leonard Göke[a,*]

[a] *Berlin University of Technology, Workgroup for Infrastructure Policy (WIP), Straße des 17. Juni 135, 10623 Berlin.*

ARTICLE INFO

Keywords:
Energy systems modelling
Open access modelling
Decarbonization
Renewable energy
Sector integration
Flexibility

ABSTRACT

Achieving climate targets requires to replace fossil fuels with renewables as a primary source of energy. This implies to extend the use of electricity generated from wind and solar beyond the power sector, either directly or indirectly via synthetic fuels. Modelling the transformation towards such an energy system is challenging, because it demands to account for fluctuations of wind and solar and the manifold ways systems can adjust to these fluctuations.

This paper introduces the anyMOD framework and its graph-based approach to address these challenges. By organizing sets in rooted trees, two features to facilitate modelling high shares of renewables and sector integration are enabled. First, the level of temporal and spatial detail can be varied by energy carrier. As a result, model size can be reduced without reducing the level of detail applied to fluctuating renewables. In addition, flexibility inherent to the system, for example in the gas network, can be accounted for. Second, substitution of energy carriers can be modelled to depend on the respective context - conversion, storage, transport or demand. This achieves an extensive representation of how flexibility can be provided in an integrated system.

1. Introduction

Mitigation of climate change requires decarbonization of the energy system. Technologically this implies to decarbonize electricity supply and, either direct- or indirectly, electrify a great share of the heat and transport sector. Since the sustainable potential of biomass and hydro is limited, intermittent renewables like wind and solar will have to provide a major share of primary energy. As a result, sectors have to be linked increasingly, and to account for these links any analysis of climate measures needs to be put into the context of the overall energy system. In the transport sector for instance, comparing electric and combustion engines highly depends on the emission intensity of the added demand for electricity [11]. If products that otherwise would require fossil fuels, are manufactured from electricity, the benefits of shifting demand or storing electricity arising from such processes has to be factored in [8]. However, while the necessity for cross-sectoral analysis grows, existing methods of energy system modelling struggle to meet the challenges high levels of sector integration and fluctuating renewables bring.

1.1. Challenges in energy system modelling

High temporal granularity is critical when modelling energy systems with large shares of renewables [33]. Former research shows that the number of representative time-steps an entire year can be reduced to without distorting model results strongly depends on the share of wind and solar generation. At low resolutions their utilization is overestimated, since fluctuations of supply cannot be captured adequately [35, 25, 17]. In addition, sectoral integration may cause a similar effect on electricity demand, if heat supply is increasingly electrified by electrical heat pumps [4]. In that case demand and efficiencies are sensitive to ambient temperature sensitive and drive fluctuations that may not be covered in a reduced time series. Since all these temporal fluctuations are weather related and thus subject to uncertainty, high temporal granularity is ideally combined with a stochastic approach [37].

At the same time, spatial aspects gain in relevance too, when modelling high levels of renewables, since their *"economic potential and generation costs depend greatly on their location"* [33]. In addition, in a renewable system the capacity of individual generation units is about a magnitude smaller than in a system characterized by thermal plants. This creates the opportunity to match demand with local supply as an alternative to transporting energy carriers over long distances [2]. However, modelling such solutions does only a require a consistent representation of relevant technologies, for instance solar home systems with batteries, but a high spatial granularity as well.

*Corresponding author.
lgo@wip.tu-berlin.de (L. Göke)

The need for temporal and spatial granularity when modelling high levels of intermittent renewables and sector integration is directly related to the concept of flexibility. Flexibility can be defined as an energy system's capability to cope with variability and uncertainty in demand [18]. The arising need for flexibility and how it can be satisfied is widely recognized as a key question for future energy systems [20, 23]. To fully account for these flexibility needs within models means to fully capture weather-driven fluctuations and consequently requires high temporal and spatial granularity.

On the other hand, including all options to provide flexibility into models calls for a detailed representation of sector integration. Many potential sources of flexibility involve complex interaction of technologies and energy carriers to build synergies between sectors [28]. To give but one example, synthetic gas can be generated from electricity via electrolysis and methanation, when supply from wind or solar exceeds demand, stored and then used to provide heat or electricity at times of low intermittent supply. Models that omit these cross-sectoral sources of flexibility might fail to identify cost-efficient solutions and excessively invest into other storage and transport capacities instead [7].

Besides these technical challenges concerning model granularity and detail, the way models are practically applied creates additional challenges that concern their temporal and spatial scope. Ideally, models can analyze how today's energy system can be transformed to comply with the climate objectives [26] set for a certain year. Therefore, their temporal scope should include multiple subsequent periods that are simultaneously optimized, also referred to as perfect foresight. If models are limited to single years, computing pathways has to rely on consecutively solving each year separately. This approach has been termed myopic foresight and found to cause suboptimal results due to stranded investments [24, 14]. A large spatial scope is valuable, because energy systems of different regions are increasingly interlinked, be it through a common energy policy or interconnected markets and networks, as for example in the European gas and electricity sector. The latter is again relevant from a flexibility perspective as well: Especially exchange of electric between regions, can even out local fluctuations of wind and solar generation [39].

Lastly, the social dimension of the energy transformation adds to the requirements on energy system models. Since they allow to assess alternative designs of the energy system in terms of costs and emissions, energy system models are capable to provide meaningful insights for energy policy to decision makers and civil society [31]. Therefore, there is a strong call for transparent or "open" models, in the sense that *"anyone is free to access, use, modify, and share"* them [27, 30]. More specifically, Weibezahn and Kendziorski [40] propose a concept of five-dimensional openness ranging from open-access publications to open data and open-source modeling languages, model code and solvers. An overlooked factor decisive to promote open models, especially beyond the scientific community, is accessibility. For organizations outside of academia, the decision to apply a model themselves or at least to critically examine its results, will greatly depend on the required effort in terms of working hours and technical knowledge.

1.2. How challenges are addressed

In this paper, the anyMOD framework is introduced to address the outlined challenges within bottom-up models of the energy system based on linear programming. Drawing on existing definitions, the term framework describes a theoretical description of the energy system that, transferred into software tools, can be used to generate specific models [15, 42].[1] Accordingly, a framework has to be provided with specific sets and how they are interrelated to create a model (e.g. technology *gas plant* produces energy carrier *electricity* from energy carrier *gas*). Adding parameter data (e.g. the efficiency of gas plants) to the model then constitutes a scenario. Working with a framework instead of a specific model allows to address a wider range of research questions since temporal, spatial and sectoral granularity and scope can both be easily adapted. In addition, novel methods implemented into the framework are also directly accessible for other researchers to use in their respective field of research.

Former research has already suggested several frameworks that serve the same purpose as anyMOD: *"to create coherent quantitative descriptions of how energy is converted, transported, and consumed"* [32] by creating and solving linear optimization problems. To serve as a reference point, in the following two of these, OSeMOSYS (short for Open Source Energy Modeling System) and Calliope, are evaluated with regard to the challenges outlined in section 1.1 [19, 32, 34]. The choice fell on these, because both are representative for a larger group of frameworks and models. OSeMOSYS is closely related to many long established tools for energy system planning like PRIMES, MESSAGE or MARKAL. The Calliope framework draws parallels to more novel tools like Balmorel, PyPSA and DIETER that are more focused on the power sector and high accuracy regarding intermittent renewables [22, 15].

These difference contexts are reflected in the way OSeMOSYS and Calliope treat time, which again affects temporal granularity. OSeMOSYS pursues an approach that aggregates an entire year into a few representative periods (e.g. a

[1] Another apt term frequently used is model generator.

summer evening). Modelling these periods instead of the full year greatly decreases computational effort, but also limits temporal granularity and thus the capability to capture fluctuations of intermittent renewables. To avoid this, Calliope does not rely on representative periods, but rather uses unaltered continuous time series.[2] This comes at the cost of a steep increase in size and solve time, if not only the electricity sector, but the entire energy system is modelled [22]. Neither of the two frameworks can account for uncertainty of supply and demand.

The use of representative periods within OSeMOSYS also restricts the modelling of storage, especially seasonal storage. If a time span, for example consider the entire summer, is reduced to one representative period, say a week, storage patterns determined for that period apply to the entire time span. Accordingly, storage levels would show the same pattern for each summer week and could not continuously increase over the course of the summer [41]. Since energy systems with high shares of variable renewables can be expected to heavily rely on storage, without major adjustments the approach is ill-suited to describe these systems [21].

Besides these differences regarding temporal granularity, both frameworks are capable to achieve high spatial granularity, since the number of regions can be chosen freely. In addition, Calliope also provides an option for discrete expansion and dispatch of technologies, which renders it appropriate for applications as detailed as the building level.

OSeMOSYS and Calliope both are suited to model sector integration, because energy carriers and technologies interacting with these carriers can be added freely. However, in both frameworks substitutability of energy carriers is restricted to conversion processes and cannot be extended to transport, storage and consumption. Considering synthetic gas and natural gas for example, both frameworks allow for technologies, like gas power plants or gas boilers that can use either one as an input, but none can reflect that both can be stored in the same facilities, transported with the same infrastructure or equally serve as feedstock for the chemical industry.

To extend the representation of technologies, OSeMOSYS supports different modes of operation, like either operating a CHP plant at a higher fuel utilization rate, but a smaller CHP coefficient or the other way round. Calliope provides a functionality to include technologies that can store a carrier for later use within a conversion, for example concentrated solar power plants that store heat for later conversion into electricity.

The temporal scope of OSeMOSYS may include multiple subsequent periods of capacity expansion to compute efficient pathways for transforming the energy system. However, properties of technologies cannot depend on their respective period of construction. As a result, technological advances, like increasing efficiency of power-to-gas technologies for instance, cannot be accounted for adequately. Calliope is limited to a single period of capacity expansion. Both frameworks support a large regional scope, since regions can be added freely.

OSeMOSYS and Callipoe are shared under an open license, provided in open languages, include freely available documentation and can be used with open solvers. While both have sparked the development of many models for various applications, OSeMOSYS seems to be more accessible, because it does not necessarily require programming experience [12].

The anyMOD framework introduced in this paper shares similarities with both OSeMOSYS and Callipoe. Like Calliope, the anyMOD framework relies on continuous time series instead of representative periods. Similar to OSeMOSYS it supports multiple periods of capacity expansion, but allows to account for technological advance and supports endogenous decommissioning of capacities. Calliopes functionality for technologies that first store and letter use a carrier is extended to the opposite case in anyMOD. Technologies might also first generate and then store a carrier. This allows to model decentralized storage systems, like a home battery paired with a photovoltaic panel, within large scale system models. Furthermore, analogous to OSeMOSYS different operational modes for technologies are supported.

Beside these gradual differences, anyMOD introduces a graph theory based approach to facilitate modelling high levels of renewables and sector integration. For this purpose, all sets are organized within a rooted tree to enable two key features:

1. The level of temporal and spatial granularity can be varied by energy carrier. For instance, electricity can be modelled hourly, while supply and demand of gas is balanced daily. This achieves the temporal granularity required to capture fluctuations in renewable electricity generation, but prevents to inflate the model, if more sectors and carriers are added. In Renaldi and Friedrich [36], a similar method from process system engineering is used to optimize a solar district heating system modelled as a linear mixed-integer problem. However, the method is only applied to the temporal granularity and to technologies instead of carriers.

[2] Using representative periods is possible as well but is not the default option.

2. Substitution of energy carriers can be modelled in dependence of the respective context: conversion, storage, transport or demand. For example, heat from residential heat pumps and district heating plants might both satisfy heat demand, but only district heat can be stored within large scale storage systems.

Unlike Calliope, anyMOD does not support discrete expansion and dispatch of technologies and therefore is not suited to be applied at the urban or building level. In addition, at this point anyMOD does not support stochastic optimization to account for weather related uncertainties of renewable generation and demand.

Like with OSeMOSYS and Calliope, code and documentation of anyMOD is freely available. It's implemented in the open source language Julia and can be used with open solvers [3]. To ensure accessibility, anyMOD does not require extensive programming skills, since models are fully defined by csv files. This also enables model development using version control to facilitate collaboration and increase transparency.

The remainder of this paper, will present in greater detail how the anyMOD features are achieved. To this end, the theoretical description of the energy system the framework builds on is explained based on a model example. First, section 2 introduces the framework's sets and how they are related to one another. Section 3 builds on this to present the equations of the actual optimization problem. In section 4 and 5 the example model is solved at different granularities and the main conclusions are drawn.

2. Definition of sets and mappings

This section discusses the sets defined within the framework, in particular time-steps, regions, energy carriers, technologies, and modes, and how they are mapped to each other. To facilitate comprehension, the whole introduction of the framework revolves around an example model. Since the primary interest of that model are not its specific results, but its general method, the choice of energy carriers and technologies considered is not exhaustive. For the same reason, some modelling assumptions that could be argued to require an in-depth technical discussion, are only treated briefly.

As a start, we introduce some concepts of graph theory and basic notations used throughout the paper. Any graph G is defined by its vertices V and edges E. A tree can be defined as a graph, where any two vertices are linked by a unique path along its vertices and edges. Distinguishing one vertex as the graph's root rt_G creates a rooted tree. The length of a path from a vertex v to the root is termed depth and provided by function $d\colon V \rightarrow \mathbb{N}_0$. Consequently, the depth of the root is always zero, which means that $d(rt_G) = 0$. All vertices on the path between a vertex v and the root are its ancestors and defined as set α_v. The descendants of a vertex v, henceforth given as δ_v, can be understood recursively: If a vertex u is an ancestor to v, v is a descendant to u. To indicate the vertex v itself should be included in a set of ancestors or descendants, we write α_v^+ or δ_v^+, respectively. The set of all ancestors or descendants of vertex v with depth z is denoted as α_v^z and δ_v^z. A subgraph of a tree that only contains the vertex v and all its descendants, is referred to as the subtree G_v. Lastly, all vertices without any descendants are called leaves. For all leaves, which are descendants of vertex v, we write λ_v. [10, 5]

2.1. Regions

Fig. 1 shows the rooted tree R organizing all regions considered within the example problem. r be an arbitrary vertex of the tree representing a region. Exemplifying the definitions and notations introduced above, the descendants of vertex *'East'* are the vertices *'East South'* and *'East North'* or $\delta_{East} = \{$*'East South'*, *'East North'*$\}$. Since both *'East South'* and *'East North'* do not have any descendants, they are leaves and $\lambda_{East} = \delta_{East}$ applies. Also, the ancestor of vertex *'West North'* at depth 1 is the vertex *'West'*, which means $\alpha^1_{WestNorth} = \{$*'West'*$\}$. The subtree at vertex *'West'* would include the vertices *'West'*, *'West North'* and *'West South'* or $V(T_{West}) = \{$*'West'*, *'West North'*, *'West South'*$\}$.

2.2. Time-steps

Analogously to regions, time-steps are organized in the rooted tree T with t representing an arbitrary vertex. In a reduced form, for the example model this tree is drawn in Fig. 2. Vertices with depth one each represent a decade, vertices with depth two correspond to all years considered within the respective decade and each year is then further dissected into daily, four-hour and finally hourly steps.

2.3. Carriers

Fig. 3 displays the rooted tree C of all energy carriers defined within the model. While the vertices *'coal'* and *'electricity'* do not have any descendants, *'heat'*, which only refers to low-temperature heat, has one descendant *'district*

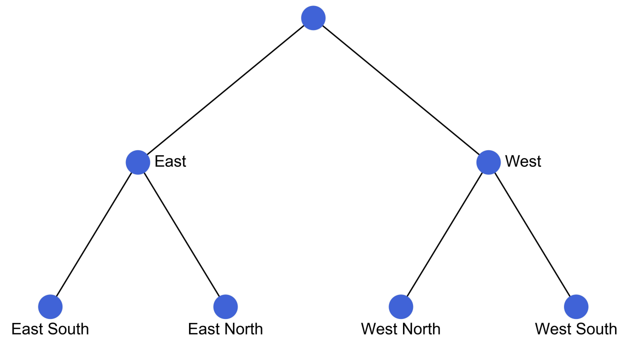

Figure 1: Rooted tree of regions in the example model

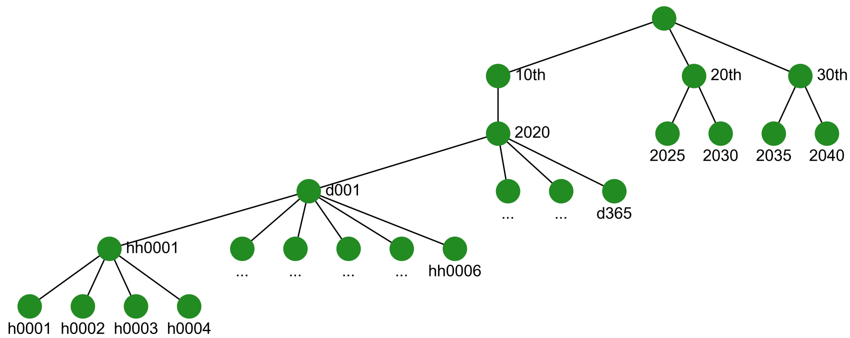

Figure 2: Rooted tree of time-steps in the example model

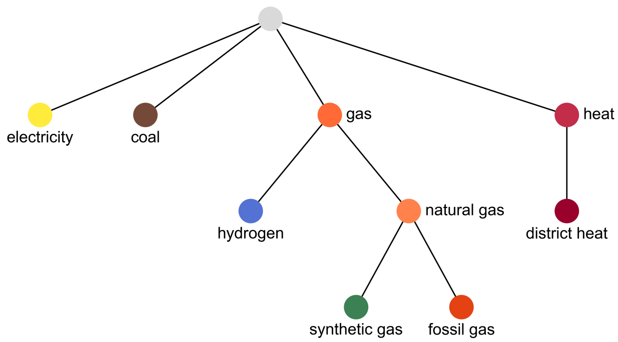

Figure 3: Rooted tree of energy carriers in the example model

heat' and gases are subdivided into *'hydrogen'* and *'natural gas'*, which again is split into *'synthetic gas'* and *'fossil gas'*. This arrangement is motivated by the fact that having carriers share a common ancestor is required for modelling them as substitutes in a certain context, as we will elaborate in section 3.

To specify the temporal and spatial granularities carriers are modelled at, each are assigned depths within the rooted trees of time-steps and regions. These is done separately for dispatch and expansion and summarized for the example model in Tab. 1.

Consequently, a depth of five for temporal dispatch of *'electricity'* means dispatch of the carrier is modelled for every time-step with depth five, which, going back to Fig. 2, corresponds to an hourly granularity. Likewise, *'heat'* and *'district heat'* are modelled at four-hour steps and all gases are balanced daily. Lastly, *'coal'* is only accounted for per

Table 1
Depths assigned to energy carriers in the example model

carrier with depth 1	carrier with depth 2	carrier with depth 3	temporal		spatial	
			dis.	exp.	dis.	exp.
electricity			5	2	1	1
heat	district heat		4	2	2	2
gas	natural gas	synthetic gas	3	2	1	1
gas	natural gas	fossil gas	3	2	1	1
gas	hydrogen		3	2	1	1
coal			2	2	1	1

year. Deciding on the temporal granularity of dispatch for a carrier is a crucial assumption on its inherent flexibility. For electricity an hourly resolution is often considered adequate when using spatially aggregated models [6]. A daily resolution for modelling gas is applied in much of the literature, since, compared to electricity, the gas network is less sensitive to temporary imbalances [16, 29]. A four-hour resolution for heat was assumed to account for the thermal inertia of buildings.

The uniform depth of two for all carrier's temporal expansion means decisions on capacity expansion are made independently for each year. If the depth were set to one instead, a decision on expansion would apply for an entire decade. In this case, expansion would be distributed equally among the decade's years yielding a linear increase in capacity. Such a setup would be suited to mimic typical polices for the expansion of wind and solar capacities.

Spatial dispatch and expansion granularity for all carriers corresponds to the regions with depth 1, namely *'West'* and *'East'*, except for *'heat'* and *'district heat'*. Here a more detailed resolution was chosen, since heat, unlike electricity or gas, cannot be transported over greater distances to offset local imbalances between supply and demand.

Certain conditions can be defined that ensure the temporal and spatial granularities assigned to each carrier are suited to create a logical consistent energy system model. anyMOD specifically checks compliance of these conditions and throws an error, if any of them is violated. To formulate these rules, the depths mapped to a specific carrier c will be termed dep_c.

First, a carrier may not be modelled at a dispatch granularity more detailed than any of its descendants, regardless if temporal or spatial. This means, the depth assigned to a specific carrier cannot exceed the smallest depth assigned to any of its descendants, as denoted in Eqs. 1a and 1b.[3]

$$dep_c^{dis,tp} \leq \min_{\hat{c} \in \delta_c} dep_{\hat{c}}^{dis,tp} \qquad \forall c \in V(C) \tag{1a}$$

$$dep_c^{dis,sp} \leq \min_{\hat{c} \in \delta_c} dep_{\hat{c}}^{dis,sp} \qquad \forall c \in V(C) \tag{1b}$$

The conditions originate from the way the framework models substitution of energy carriers. As section 3 will explain in detail, this is achieved by aggregating variables of descendant carriers with the ancestral carrier. However, such an aggregation is impossible, if for example the ancestral carrier has an hourly resolution, but one of its descendants is modelled daily.

The second group of conditions addresses the relation between dispatch and expansion granularity. As stated in Eq. 2, the spatial granularity of expansion may not be less detailed than the spatial granularity of dispatch for any carrier or, in terms of depths, the depth of dispatch cannot exceed the depth of expansion.

$$dep_c^{exp,sp} \geq dep_c^{dis,sp} \qquad \forall c \in V(C) \tag{2}$$

This condition is necessary to ensure each dispatch variable in the model can be mapped to a corresponding capacity. If, for instance, expansion is modelled at the country level, but dispatch considered separately for each state within the country, assigning a capacity to each of these states would not be possible. The opposite case with dispatch on the country level but regional expansion is supported and leads to an aggregation of regional capacities by country.

For the same reason a similar condition on temporal granularities is required. This condition states that for any carrier the temporal granularity of expansion may not be more detailed than the temporal granularity of dispatch. As

[3]The hat operator is used throughout the paper to indicate a vertex is a descendant to another vertex within the same equation.

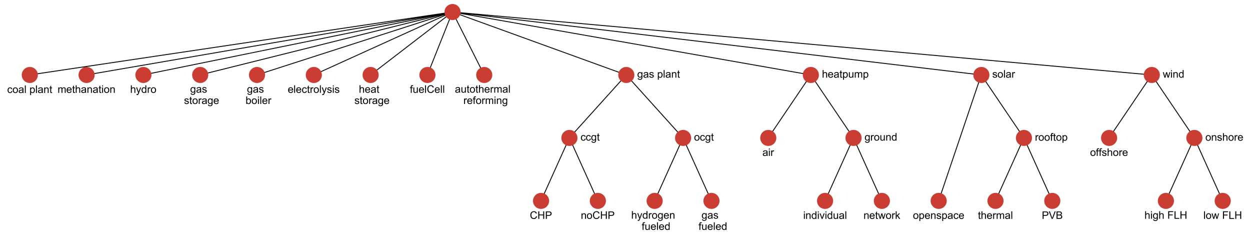

Figure 4: Rooted tree of technologies in the example model

formulated in Eq. 3, this implies the depth assigned for dispatch cannot exceed the depth of expansion.

$$dep_c^{exp,tp} \leq dep_c^{dis,tp} \qquad \forall c \in V(C) \tag{3}$$

If, in violation of Eq. 3, capacity expansion had an daily resolution, but dispatch were only modelled yearly, again a sensible assignment of capacity to dispatch variables would not be possible.

Besides granularities for dispatch and expansion, modelling also requires a resolution that connects those two. Usually models do this at a yearly resolution. This implies installed capacities do not vary within a year and dispatch decisions of different years do not affect one another. For instance, a cyclic condition usually enforces the same storage levels at the beginning and end of one year. Within the framework, this granularity connecting dispatch and expansion will be termed the superordinate granularity or depth of dispatch dep^{sup}. Since Eq. 3 considers each carrier separately, so far this granularity could also vary by energy carrier. Although such an approach is technically feasible, it would greatly complicate the interpretation of results and does not appear practical. Therefore, Eq. 3 is re-written into Eq. 4, which applies the same condition to all carriers at once instead of separately.

$$dep^{sup} = \max_{c \in V(C)} dep_c^{exp,tp} \leq \min_{c \in V(C)} dep_c^{dis,tp} \tag{4}$$

All time-steps of depth dep^{sup} are termed Φ or superordinate dispatch time-steps. Each subordinate dispatch time-step t has exactly one ancestor within Φ, which is referred to as α_t^{sup}. In the example model dep^{sup} is two and consequently Φ corresponds to all years. For any hour or day t, α_t^{sup} assigns the year the respective day or hour is in.

2.4. Technologies

Technologies are organized in the rooted tree E, which is shown in Fig. 4 for the example model. Only leaves of this tree correspond to actual technologies, while all other vertices serve the sole purpose of organizing them. For instance, to reflect how photovoltaic and solar thermal rooftop systems compete for a limited amount of rooftop area, their shared ancestor *'rooftop'* can be used to enforce an upper limit on the sum of their capacities. Also, parameter values shared by several technologies with the same ancestor, like the availability time-series for solar technologies, only have to be read-in once and will be inherited by all descendants.

The function $g(e)$ maps technologies to one of three groups: *stock*, *mature* and *emerging*. Stock technologies cannot be expended and are limited to pre-existing capacities. Emerging technologies distinguishes from mature technologies that capacities are differentiated by time-step of construction. In the case of electrolyzers for example, substantial increases in efficiency are expected until 2050. To account for such improvements, capacities build in different years have to be considered separately. For other technologies, no substantial advances are expected and such differentiation would only cause an unnecessary increase in model size.

Generated and used carriers are mapped to technologies by the sets γ_e^{gen} and γ_e^{use}, respectively. Any used carrier c cannot be a descendant to another used carrier c'. The condition applies to generated carriers analogously and both conditions are formalized by Eqs. 5a and 5b.

$$c \notin \delta_{c'} \quad \forall e \in V(E), (c, c') \in \{\gamma_e^{use} \times \gamma_e^{use} \mid c \neq c'\} \tag{5a}$$
$$c \notin \delta_{c'} \quad \forall e \in V(E), (c, c') \in \{\gamma_e^{gen} \times \gamma_e^{gen} \mid c \neq c'\} \tag{5b}$$

Considering the combined-cycle gas power plant (CCGT) with cogeneration (CHP) from the example, *'natural gas'* is converted to *'district heat'* and *'electricity'*, hence $\gamma_{CHP}^{use} = \{\textit{'natural gas'}\}$ and $\gamma_{CHP}^{gen} = \{\textit{'district heat'}, \textit{'electricity'}\}$.

Additionally assigning *'fossil gas'* as a used carrier would pose a logical contradiction since *'natural gas'* implicitly already includes its descendant *'fossil gas'* and consequently violate Eq. 5a.

Charged carriers are denoted as γ_e^{stI}; discharged carriers are referred to as γ_e^{stO}. By default, only carriers, which are leaves, can be explicitly stored. If a technology is defined to store a non-leaf carrier c, actually stored are only its leaves λ_c. For instance, in the example *gas storage* is defined to store *gas* which means the technology can equally store *hydrogen*, *synthetic gas* and *fossil gas*. Deviating from this approach gives rise to unintended effects.[4] To elucidate this, assume *gas storage* would directly store the carrier *gas* instead. Since descendants are included in the ancestors energy balance, *hydrogen* could still be charged. However, it would be discharged as *gas* and could not be used wherever *hydrogen* is specifically required.

The representation of storage is not limited to charging and discharging carriers from external sources, but can also account for carriers generated or used by the same technology. To clarify this, we assume a carrier c is an element of γ_e^{stO}, but not within γ_e^{stI}. This implis it can be discharged, but not charged from an external source. However, if c is also an element of γ_e^{gen}, it can be charged by the the technologies own generation instead. For instance, the photovoltaic battery system (PVB) in the example represents a photovoltaic panel combined with a home battery. In line with other research, we assume home batteries cannot be charged from the grid, but can provide electricity to the grid [38]. Therefore, *'electricity'* is an element of γ_{PVB}^{gen} and γ_{PVB}^{stO}, but γ_{PVB}^{stI} is empty. Nevertheless, the battery can still be charged by the system's own generation from the photovoltaic panel. Correspondingly, a charged carrier can be discharged internally if within γ_e^{use}. In this case, an industrial furnace provided with gas by an on-site gas storage could serve as an example. If carriers are charged or discharged internally, also non-leaf carriers can be stored.

Applying this, 6 and 7 define sets of stored carriers for an technology e. All carriers charged and discharged externally are provided by γ_e^{stEx}. This set is unified with all carriers carrier charged externally and discharged internally as well as the other way around, to obtain all carriers stored γ_e^{st}.

$$\gamma_e^{stEx} = \overbrace{\{\lambda_c \,:\, c \in \gamma_e^{stO} \cup \gamma_e^{stI}\}}^{\text{external charging or discharging}} \tag{6}$$

$$\gamma_e^{st} = \gamma_e^{stEx} \cup \underbrace{(\gamma_e^{gen} \cup \gamma_e^{stO})}_{\text{internal charging}} \cap \underbrace{(\gamma_e^{use} \cap \gamma_e^{stI})}_{\text{internal discharging}} \tag{7}$$

The sets γ_e^{in} and γ_e^{out} collect all external in- and output carriers of a technology e:

$$\gamma_e^{in} = \gamma_e^{use} \cup \gamma_e^{stEx} \tag{8a}$$

$$\gamma_e^{out} = \gamma_e^{gen} \cup \gamma_e^{stEx} \tag{8b}$$

In addition, all technologies any conversion or storage carrier was assigned to are collected within the respective sets Γ^{cv} and Γ^{st}, which are defined by the following equations:

$$\Gamma^{cv} = \{V(E) \,|\, \gamma_e^{gen} \cup \gamma_e^{use} \neq \emptyset\} \tag{9a}$$

$$\Gamma^{st} = \{V(E) \,|\, \gamma_e^{st} \neq \emptyset\} \tag{9b}$$

The directed graph in Fig. 5 summarizes how in- and output carriers are mapped to technologies in the example model. In the graph all technologies are symbolized by grey vertices. Their entering edges relate to inputs γ_e^{in}; outgoing edges to outputs γ_e^{out}. Carriers are symbolized by colored vertices that have outgoing edges directed towards their ancestors. The graph demonstrates, how organizing carriers in rooted trees supports modelling the manifold ways energy carriers can be substituted and interact with technologies in an integrated energy system: Synthetic gas has to be created from hydrogen, which again requires the use of electricity via electrolysis, while natural gas cannot be created from other carriers. However, both energy carriers can equally fuel gas boilers and power plants or be used for auto thermal reforming, a gas-based process to create hydrogen. Also, any of these carriers can be stored in a gas storage system, since *gas* is an ancestor to all of them.

Although the example model focuses on the interplay of gas-based fuels to demonstrate the capabilities of the presented method, it can be applied beyond: For instance, processes in the energy-intensive industry often require

[4]It can be explicitly enforced though, but this a special case not discussed within the paper.

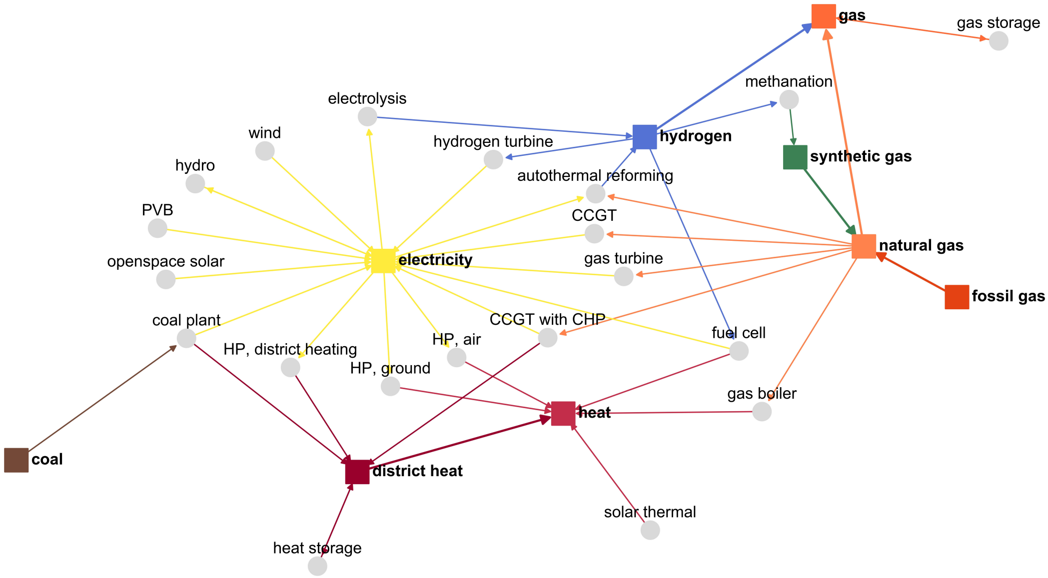

Figure 5: Qualitative energy flow graph for example model

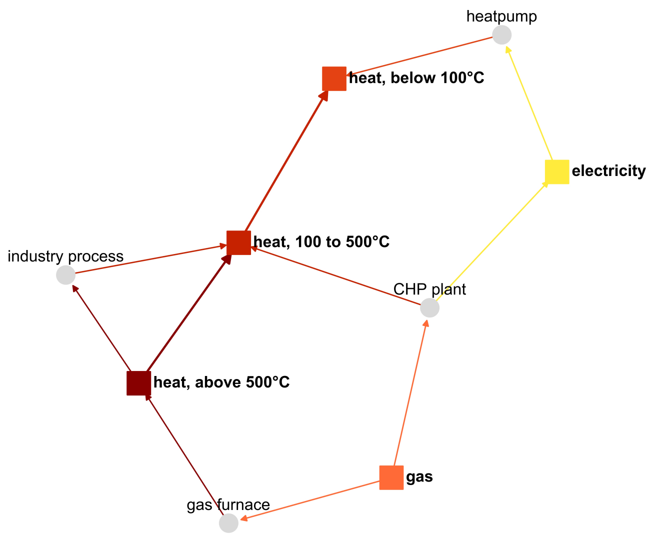

Figure 6: Qualitative energy flow graph for alternative application

high-temperature heat at different levels, which makes decarbonization challenging [1]. However, providing a process with heat on a temperature level that exceeds its requirements is possible. Also excess heat from one process can server as input to another. The qualitative energy flow diagram in Fig. 6 outlines how these aspects could be accounted for within energy system models by the introduced method. Since the carrier *'heat, above 500°C'* is a descendant of *'heat, 100 to 500°C'* and *'heat, below 100°C'*, in contrast to the other technologies *'gas furnace'* is able to satisfy demand on all levels. Also, a process that requires heat at the highest temperature level and provides excess heat again at a lower level, can be modelled.

2.5. Modes

The rooted tree M organizes the different operational modes m defined within the framework. In contrast to the other graphs, the rooted tree of modes is trivial, meaning it only consists out of the root and its direct descendants. The set μ_e maps its operational modes to each technology or, if only one mode exists, just assigns the root rt_M. In the

Nomenclature

Basic definitions

rt_G	root of tree G
α_v, α_v^+	ancestors of vertex v, + includes v
α_v^z	ancestors of vertex v at depth z
δ_v, δ_v^+	descendants of vertex v, + includes v
δ_v^z	descendants of vertex v at depth z
λ_v	leaves descendant to v

Functions and mappings

$d(v)$	depth of vertex v
dep_c	depth assigned to carrier c
dep_{sup}	depth of superordinate dispatch time-steps
$s(t)$	scaling factor for capacities at time-step t
$g(e)$	type assigned to technology e

Parameter

$ava^{cv}_{t,\tilde{t},r,e,m}$	availability of conversion capacity
$ava^{stI/stO/stL}_{t,\tilde{t},r,c,e,m}$	availability of storage capacity
$eff^{cv}_{t,\tilde{t},r,e,m}$	efficiency of conversion process
$eff^{stI/stO}_{t,\tilde{t},r,c,e,m}$	efficiency of charging/discharging
$eff^{exc}_{t,r,r',c}$	efficiency of energy exchange
$ratio^{out,eq}_{t,\tilde{t},r,c,e,m}$	fixed share of carrier c on total output
$in_{t,\tilde{t},r,c,e,m}$	inflows into storage system
$dis_{t,\tilde{t},r,c,e,m}$	self-discharge rate of storage
$dem_{\hat{t},\hat{r},\hat{c}}$	energy demanded
$cap^{buy/sell}_{t,r,c,i}$	capacity for buying/selling

Sets

Ω	all possible indices for dispatch variables of technologies
$\Gamma^{cv/st}$	technologies converting/storing carriers
$\Psi_e^{in/out}$	pairs defining capacity constraints on conversion input/output
$\gamma_e^{use/gen}$	carriers used/generated by technology e
γ_e^{stEx}	carries stored explicitly and externally
γ_e^{stCap}	carries assigned to storage capacity
γ_e^{st}	all carriers stored explicitly
$\gamma_e^{in/out}$	external input/output carriers
μ_e	modes assigned to technology e
τ_c	dispatch time-steps
ρ_c	dispatch regions
φ_c	pairs of dispatch time-steps and regions
$\sigma_{\hat{c},r,t}$	pairs of dispatch time-steps and regions aggregated to determine dispatch of $\hat{c}$ at time-step t in region r
$\theta^{dis}_{e,\tilde{t}}$	time-steps of construction considered dispatched separately
$\theta^{exp}_{e,t,\tilde{t}}$	time-steps of construction aggregated to obtain capacity
$\beta_{c,r}$	region with that region r can exchange carrier c
$\zeta^{buy/sell}_{t,r,c,i}$	steps in supply/demand curve for trade
$\omega^{cv/st}_{t,\tilde{t},r,e}$	set of modes, each set requires an individual conversion/storage balance
$\eta_e^{tp/sp}$	time-steps/regions of capacity expansion

Variables

$Te^{cv/st}_{\hat{t},\hat{r},\hat{c}}$	net output of conversion/storage
$Exc^{net}_{\hat{t},\hat{r},\hat{c}}$	net exchange
$Trd^{net}_{\hat{t},\hat{r},\hat{c}}$	net trade
$Cv^{in/out}_{t,\tilde{t},r,c,e,m}$	aggregated conversion input/output
$St^{in/out}_{t,\tilde{t},r,c,e,m}$	aggregated storage input/output
$Gen_{t,\tilde{t},r,c,e,m}$	generated energy
$Use_{t,\tilde{t},r,c,e,m}$	used energy
$StO^{ext/int}_{t,\tilde{t},r,c,e,m}$	externally/internally discharged energy
$StI^{ext/int}_{t,\tilde{t},r,c,e,m}$	externally/internally charged energy
$StLvl_{t,\tilde{t},r,c,e,m}$	storage level
$Exc_{t,r,r',c}$	energy exchange from region r to region r'
$Trd^{buy/sell}_{t,r,c,i}$	bought/sold energy
$Cap^{opr/ist,cv}_{t,\tilde{t},r,e}$	operated/installed conversion capacity
$Cap^{opr/ist,stI}_{t,\tilde{t},r,e,c}$	operated/installed storage input capacity
$Cap^{opr/ist,stO}_{t,\tilde{t},r,e,c}$	operated/installed output storage capacity
$Cap^{opr/ist,stS}_{t,\tilde{t},r,e,c}$	operated/installed storage size
$Cap^{opr/ist,exc}_{t,r,r',c}$	operated/installed exchange capacity
$Exp^{cv}_{t,r,e}$	expansion of conversion capacity
$Exp^{stI}_{t,r,c,e}$	expansion of storage input capacity
$Exp^{stO}_{t,r,c,e}$	expansion of storage output capacity
$Exp^{stS}_{t,r,c,e}$	expansion of storage size
$Exp^{exc}_{t,r,r',c}$	expansion of exchange capacity

example model, distinct modes termed *more heat* and *more electricity* are only defined for CCGT plants with CHP. The *more Heat* mode operates at a higher fuel utilization rate, but a smaller CHP coefficient.

3. Formulation of optimization problem

Building on the sets and mappings introduced in the former section, the constraints of model's underlying optimization can be formulated. We will start with dispatch related constraint, followed by capacity constraints, which connect dispatch and expansion and close with the equations to describe expansion itself. Since the cost minimizing objective function does not substantially differ to pre-existing models, it is provided in Appendix B. The same applies for constraints that only impose endogenous limits on variables.

3.1. Energy balance

The energy balance ensures demand for each carrier c equals or does not exceed its supply at any time t or place r. To model this, all dispatch time-steps τ_c and regions ρ_c of a carrier c are defined as follows:

$$\tau_c = \{V(T) \mid d(t) = dep_c^{dis,tp}\} \tag{10a}$$

$$\rho_c = \{V(R) \mid d(r) = dep_c^{dis,sp}\} \tag{10b}$$

Consequently, the cartesian product of τ_c and ρ_c gives the temporal and spatial granularity φ_c that a carrier c is modelled at.

$$\varphi_c = \tau_c \times \rho_c \tag{11}$$

Since demand for a carrier c can not only be met by the carrier itself, but also by any of its descendants $\hat{c}$, these have to be included into the energy balance as well. However, according to Eq. 1a and 1b, these descendants might be modelled at a granularity more detailed than the carrier itself. Therefore, elements of these descendants have to be aggregated to comply with the resolution of the ancestral carrier. When balancing the time-step t, the dispatch time-steps of a descendant carrier $\hat{c}$ that require aggregation, correspond to the intersection of descendant carriers time-steps $\tau_{\hat{c}}$ with the descendants of the balanced time-step δ_t^+. The same reasoning is applied to regions and the set of pairs $\sigma_{\hat{c},r,t}$ can be obtained. As defined by Eq. 12, this set contains all time-steps and regions that have to be aggregated to account for dispatch of a carrier $\hat{c}$ at time-step t in region r.

$$\sigma_{\hat{c},r,t} = \tau_{\hat{c}} \cap \delta_t^+ \times \rho_{\hat{c}} \cap \delta_r^+ \tag{12}$$

The equation applies as well, if t or r are already at the right granularity, because the set δ_v^+ by definition also includes the vertex v itself.

To enable descendant carriers to satisfy demand, by default the energy balance is not an equality constraint and supply might exceed demand. The carriers *district heat* and *heat* from the example model can be used to illustrate this. To let the model endogenously decide weather to use district heating technologies or not, demand was only specified for the ancestral carrier *heat*.[5] As a result, formulating the energy balance for *district heat* as an equality constraint, would fix its generation to zero. If overall generation of a carrier should actually be limited to its demand, alternatively an equality constraint can be enforced for specific carriers. Building on this, the energy balance is formulated in eqn. 13. To facilitate the understanding, optimization variables start with a uppercase letter, while parameters are written in lowercase.

$$\sum_{\hat{c} \in \delta_c^+} \sum_{\langle \hat{t},\hat{r} \rangle \in \sigma_{t,r,\hat{c}}} \underbrace{Te^{cv}_{\hat{t},\hat{r},\hat{c}} + Te^{st}_{\hat{t},\hat{r},\hat{c}}}_{\text{supply and demand by technologies}} + \overbrace{Exc^{net}_{\hat{t},\hat{r},\hat{c}}}^{\text{exchange with other regions}} + \underbrace{Trd^{net}_{\hat{t},\hat{r},\hat{c}}}_{\text{trade with exogenous markets}} - \overbrace{dem_{\hat{t},\hat{r},\hat{c}}}^{\text{exogenous demand}} \geq 0 \qquad \forall c \in V(C),\ \langle t,r \rangle \in \varphi_c \tag{13}$$

Conversion related dispatch variables are summarized by Te^{cv} and include Gen for generation and Use for use. Analogously, Te^{st} is composed of StI^{ext} and StO^{ext} to account for external in- and output of storage. Each of these variables is specified for five different dimensions: time-step of dispatch t, region r, carrier c, mode m and lastly time-step of construction $\tilde{t}$. The cartesian product of all dimensions is denoted as Ω.

[5] In the example, an upper limit on the generation of district heat for each time-step reflects that only a share of consumers can be connected to a district heating network.

For stock and mature technologies, which are not differentiated by time-step of construction, $\tilde{t}$ always corresponds to the root of the time-step tree rt_T. In case of an emerging technology e, all time-steps of construction that result in a life-span, which includes the dispatch time-step t, have to be considered seperately. To elucidate this, consider the time-steps as defined in the example problem and a technology with a constant lifetime $lt_{e,\tilde{t}}$ of 15 years. For any dispatch time-step t within the year 2020, only capacities constructed in 2020 have to be considered. However, if t is within 2050 instead, the construction time-steps 2040 and 2045 have to considered in addition to 2050. In conclusion, Eq. 14 defines the set $\theta^{dis}_{e,t}$ that provides the construction time-steps to consider separately for a dispatch variable of technology e at dispatch time-step t.

$$\theta^{dis}_{e,\tilde{t}} = \begin{cases} \{r_T\} & \text{,if } g(e) = \textit{`mature'} \vee g(e) = \textit{`stock'} \\ \{\tilde{t}' \in \Phi \mid \tilde{t}' \in (\alpha^{sup}_t - lt^{tech}_{e,\tilde{t}'}, \alpha^{sup}_t]\} & \text{,if } g(e) = \textit{`emerging'} \end{cases} \tag{14}$$

Dispatch variables for all conversion and storage technologies are summed by time-steps of construction $\tilde{t}$ and modes m to define Te^{cv} and Te^{st} as denoted in Eqs. 15a and 15b. Iverson brackets are used to indicate that dispatch variables are only created, if the respective carrier is actually assigned to the technology.

$$Te^{cv}_{t,r,c} = \sum_{e\in\Gamma^{cv}} \sum_{\tilde{t}\in\theta^{dis}_{e,t}} \sum_{m\in\mu_e} Gen_{t,\tilde{t},r,c,e,m}[c \in \gamma^{gen}_e] - Use_{t,\tilde{t},r,c,e,m}[c \in \gamma^{use}_e] \qquad \forall c \in V(C),\ \langle t,r\rangle \in \varphi_c \tag{15a}$$

$$Te^{st}_{t,r,c} = \sum_{e\in\Gamma^{st}} \sum_{\tilde{t}\in\theta^{dis}_{e,t}} \sum_{m\in\mu_e} StO^{ext}_{t,\tilde{t},r,c,e,m}[c \in \gamma^{stEx}_e] - StI^{ext}_{t,\tilde{t},r,c,e,m}[c \in \gamma^{stEx}_e] \qquad \forall c \in V(C),\ \langle t,r\rangle \in \varphi_c \tag{15b}$$

In the energy balance, $Exc^{net}_{\hat{t},\hat{r},\hat{c}}$ refers to net imports of region $\hat{r}$ from other regions. The set $\beta_{c,r}$ includes all regions with that region r can exchange carrier c. Exchange can be considered similar to storage, since both shift energy, one in space and the other in time. Therefore, similar to storage, exchange of carriers is always limited to leaves, because otherwise the same effects as described for storage earlier will occur. For instance, to represent the gas network in the example, $\beta_{c,r}$ is defined for *gas*. Consequently, only the carriers *hydrogen*, *synthetic gas* and *fossil gas* are explicitly exchanged.

Applying this, Eq. 16 computes the net import based on the exchange variables Exc and the efficiency of exchange eff^{exc} that accounts for exchange losses. The first region in the index always refers to the region energy is being transported to and the second to the region it is being transported from.

$$Exc^{net}_{t,r,\hat{c}} = \sum_{r'\in\beta_{c,r}} \sum_{\hat{r}'\in\rho_{\hat{c}}\cap\delta^+_{r'}} \frac{Exc_{t,\hat{r},\hat{r}',c}}{1/eff^{exc}_{t,\hat{r},\hat{r}',\hat{c}}} - Exc_{t,\hat{r}',\hat{r},\hat{c}} \ \forall\langle c,r\rangle \in \{V(C)\times V(R) \mid \beta_{c,r}\},\ \hat{c} \in \lambda_c,\ t \in \tau_{\hat{c}},\ \hat{r} \in \rho_{\hat{c}}\cap\delta^+_r \tag{16}$$

Just as explained at the beginning of the section, the region specified in $\beta_{c,r}$ might be less detailed than the regions a descendant carrier $\hat{c}$ is modelled for. Therefore, exchange variables are aggregated by regions using the same approach introduced for technologies earlier.

The net effect of trade is accounted for in the energy balance by Trd^{net} defined in Eq. 17. In contrast to exchange, trade refers to buying or selling carriers to an exogenous market at a fixed price. The quantity that can be bought or sold at a given price can be limited, which can be used to create a stepped supply or demand curve. Each of these steps is denoted as ζ^{buy} or ζ^{sell}, respectively.

$$Trd^{net}_{t,r,c} = \sum_{i\in\zeta^{buy}} Trd^{buy}_{t,r,c,i} - \sum_{i\in\zeta^{sell}} Trd^{sell}_{t,r,c,i} \qquad \forall c \in V(C),\ \langle t,r\rangle \in \varphi_c \tag{17}$$

Potential applications of this functionality range from a representation of global commodity markets to accounting for price-elastic demand in the electricity sector. The last remaining element of the energy balance dem is an exogenously set parameter and refers to inelastic demand.

3.2. Conversion balance

The conversion balance describes how technologies transform energy carriers into one another. For this purpose, the in- and outputs to the conversion process are summarized by carrier as Cv^{in} and Cv^{out}, which are defined in Eqs.

18a and 18b. As set out in section 2.4, these in- and outputs are not limited to use and generation variables, but can also include internal storage variables.

$$Cv^{in}_{t,\tilde{t},r,c,e,m} = Use_{t,\tilde{t},r,c,e,m} + StO^{int}_{t,\tilde{t},r,c,e,m}[c \in \gamma^{stO}_{e}] \quad \forall e \in V(E),\, c \in \gamma^{use}_{e},\langle t,\, r\rangle \in \varphi_c,\, \tilde{t} \in \theta^{dis}_{e,t},\, m \in \mu_e \tag{18a}$$

$$Cv^{out}_{t,\tilde{t},r,c,e,m} = Gen_{t,\tilde{t},r,c,e,m} + StI^{int}_{t,\tilde{t},r,c,e,m}[c \in \gamma^{stI}_{e}] \quad \forall e \in V(E),\, c \in \gamma^{gen}_{e},\, \langle t, r\rangle \in \varphi_c,\, \tilde{t} \in \theta^{dis}_{e,t},\, m \in \mu_e \tag{18b}$$

Only technologies that are assigned both, used and generated carriers, require a conversion balance. Conversion is balanced at the least detailed granularity of all carriers involved in the conversion process. Otherwise, a carrier with a less detailed granularity could not be accounted for. Applying this, Eq. 19 defines the resolution of the energy balance for each technology e.

$$\epsilon_e = \{V(T) \,|\, d(t) = \min_{c \in \gamma^{gen}_{e} \cup \gamma^{use}_{e}} dep^{dis,tp}_{c}\} \times \{V(R) \,|\, d(r) = \min_{c \in \gamma^{gen}_{e} \cup \gamma^{use}_{e}} dep^{dis,sp}_{c}\} \tag{19}$$

The overall efficiency of a conversion process that determines the ratio between in- and output quantities is denoted as eff^{cv}. If a technology's conversion efficiency differs by operational mode, each of these modes has to be considered by a separate equation. Therefore, ω^{cv} provides all sets of modes that require an individual energy balance. On this basis, the conversion balance given by Eq. 20 can be formed.

$$\sum_{m \in \xi} eff^{cv}_{t,\tilde{t},r,e,m} \sum_{c \in \gamma^{use}_{e}} \sum_{\langle \hat{t},\hat{r}\rangle \in \sigma_{t,r,c}} Cv^{in}_{\hat{t},\tilde{t},\hat{r},c,e,m} = \sum_{m \in \xi} \sum_{c \in \gamma^{gen}_{e}} \sum_{\langle \hat{t},\hat{r}\rangle \in \sigma_{t,r,c}} Cv^{out}_{\hat{t},\tilde{t},\hat{r},c,e,m}$$
$$\forall e \in \{V(E) \,|\, \gamma^{use}_{e} \neq \emptyset \wedge \gamma^{gen}_{e} \neq \emptyset\},\, \langle t, r\rangle \in \epsilon_e, \tilde{t} \in \theta^{dis}_{e,t},\, \xi \in \omega^{cv}_{t,\tilde{t},r,e} \tag{20}$$

For the CCGT plant with CHP from the example, the conversion balance is created daily and for each region of depth one, which corresponds to the granularity of its less detailed carrier *gas*. In addition, separate balances are created for each operational mode, since these differ in terms of efficiency, which means $\omega^{cv} = \{\{\textit{'more heat'}\}, \{\textit{'more electricity'}\}\}$.

3.3. Storage balance

The storage balance connects in- and output of a storage system to the storage level. The in- and output to the storage are compromised of external and internal storage variables as defined in Eq. 21.

$$St^{in}_{t,\tilde{t},r,c,e,m} = StI^{ext}_{t,\tilde{t},r,c,e,m}[c \in \gamma^{stEx}_{e}] + StI^{int}_{t,\tilde{t},r,c,e,m}[c \in \gamma^{gen}_{e}] \quad \forall e \in V(E),\, c \in \gamma^{st}_{e},\, \langle t, r\rangle \in \varphi_c,\, \tilde{t} \in \theta^{dis}_{e,t},\, m \in \mu_e \tag{21a}$$

$$St^{out}_{t,\tilde{t},r,c,e,m} = StO^{ext}_{t,\tilde{t},r,c,e,m}[c \in \gamma^{stEx}_{e}] + StO^{int}_{t,\tilde{t},r,c,e,m}[c \in \gamma^{use}_{e}] \quad \forall e \in V(E),\, c \in \gamma^{st}_{e},\, \langle t, r\rangle \in \varphi_c,\, \tilde{t} \in \theta^{dis}_{e,t},\, m \in \mu_e \tag{21b}$$

In Eq. 22 the storage level $StLvl$ at time-step t is computed by summing levels of the previous time-step $t-1$ with storage in- and outputs. To a enforce a cyclic condition, the previous time-step to the first time-step is the last time-step within the same superordinate dispatch time-step (e.g. for *h0001* in *2020* the previous time-step is *h8760* in *2020*).

$$\overbrace{\sum_{m \in \xi} StLvl_{t,\tilde{t},r,c,e,m}}^{\text{current level}} = \overbrace{\sum_{m \in \xi} \frac{StLvl_{t-1,\tilde{t},r,c,e,m}}{1 - dis_{t,\tilde{t},r,c,e,m}}}^{\text{loss adjusted previous level}} \overbrace{+ in_{t,\tilde{t},r,c,e,m} + \frac{St^{in}_{t,\tilde{t},r,c,e,m}}{1/eff^{stI}_{t,\tilde{t},r,c,e,m}}}^{\text{storage inputs}} - \overbrace{\frac{St^{out}_{t,\tilde{t},r,c,e,m}}{eff^{stO}_{t,\tilde{t},r,c,e,m}}}^{\text{storage outputs}} \tag{22}$$
$$\forall e \in \Gamma^{st},\, c \in \gamma^{st}_{e},\, \langle t, r\rangle \in \varphi_c,\, \tilde{t} \in \theta^{dis}_{e,t},\, \xi \in \omega^{st}_{t,\tilde{t},r,e}$$

In the storage balance, dis refers to the self-discharge rate, while eff^{stI} and eff^{stO} account for losses associated with charging and discharging. Similar to the conversion balance ω^{st} provides all sets of modes that require an individual balance. Lastly, the parameter in allows to account for external inputs into the storage system, for instance inflows into hydro reservoirs.

3.4. Ratio constraints

Ratios among in- and output carriers can be restricted by an equality, greater-than or less-than constraint. Since all constraints on in- or output ratios are structured the same, only the equality constraint on output carries is formulated in Eq. 23.

$$\underbrace{\sum_{\langle \hat{t},\hat{r}\rangle \in \sigma_{t,r,c}} Cv^{out}_{\hat{t},\tilde{t},\hat{r},c,e,m}}_{\text{output of restricted carrier}} = ratio^{out,eq}_{t,\tilde{t},r,c,e,m} \underbrace{\sum_{c' \in \gamma^{out}_{e}} \sum_{\langle \hat{t},\hat{r}\rangle \in \sigma_{t,r,c'}} Cv^{out}_{\hat{t},\tilde{t},\hat{r},c',e,m}}_{\text{output of all carriers}} \quad \forall \langle t,\tilde{t},r,c,e,m\rangle \in \{\Omega \mid ratio^{out,eq}_{t,\tilde{t},r,c,e,m}\} \tag{23}$$

The parameter $ratio^{out,eq}$ specifies a carrier's share of the total output. In the example, it is defined for the share of electricity in total outputs of CCGT plants with CHP, coal plants and fuel cells. Accordingly, only in these cases the corresponding constraints are created.

3.5. Capacity constraints

Dispatch variables are constrained to not exceed the operating capacities Cap^{opr}. To compare dispatch expressed in energy units with capacities, which are expressed in power units, dispatch variables are corrected for the length of the respective dispatch time-step. To this end we define the function s that assign a correction factor $s(t)$ for each time-step t. As explained in section 2.3, expansion can be modelled with greater spatial detail than dispatch and as a result comparing expansion with dispatch requires aggregation. For this purpose, expansion regions of technology e are termed η^{sp}_{e} and by default their resolution corresponds to the most detailed resolution across all carriers assigned, as expressed in Eq. 24.

$$\eta^{sp}_{e} = \{V(R) \mid d(r) = \max_{c \in \gamma^{in}_{e} \cup \gamma^{out}_{e}} (dep^{exp,sp}_{c})\} \tag{24}$$

Since conversion capacities transform carriers modelled at different granularities, the question arises at which resolution capacity constraints should be enforced. To answer this, part A of the appendix introduces an algorithm that determines the smallest set of constraints required for dispatch variables to comply with the operated capacities $Cap^{opr,cv}$. For each technology e this set is referred to as Ψ_{e} and be can be split into in- and output. The corresponding constraints are provided by Eqs. 25a and 25b.

$$s(t) \sum_{c \in \kappa} \sum_{\langle \hat{t},\hat{r}\rangle \in \sigma_{t,r,c}} \sum_{m \in \mu_{e}} \frac{Cv^{in}_{\hat{t},\tilde{t},\hat{r},c,e,m}}{ava^{cv}_{\hat{t},\tilde{t},\hat{r},e,m}} \leq \sum_{\hat{r} \in \eta^{sp}_{e} \cap \delta^{+}_{r}} Cap^{opr,cv}_{\alpha^{sup}_{t},\tilde{t},\hat{r},e} \quad \forall e \in \Gamma^{cv},\ \langle \kappa,t,r\rangle \in \Psi^{in}_{e},\ \tilde{t} \in \theta^{dis}_{e,t} \tag{25a}$$

$$s(t) \sum_{c \in \kappa} \sum_{\langle \hat{t},\hat{r}\rangle \in \sigma_{t,r,c}} \sum_{m \in \mu_{e}} \frac{Cv^{out}_{\hat{t},\tilde{t},\hat{r},c,e,m}}{ava^{cv}_{\hat{t},\tilde{t},\hat{r},e,m}\ eff^{cv}_{\hat{t},\tilde{t},\hat{r},e,m}} \leq \sum_{\hat{r} \in \eta^{sp}_{e} \cap \delta^{+}_{r}} Cap^{opr,cv}_{\alpha^{sup}_{t},\tilde{t},\hat{r},e} \quad \forall e \in \Gamma^{cv},\ \langle \kappa,t,r\rangle \in \Psi^{out}_{e},\ \tilde{t} \in \theta^{dis}_{e,t} \tag{25b}$$

In anyMOD capacities of technologies generally refer to input capacities, which is why the constraint on output capacity in Eq. 25b has to account for the respective efficiency.

For storage, capacity constraints are separately enforced for storage input stI, storage output stO and storage size stS. All storage carriers initially assigned to a technology are denoted as γ^{stCap}_{e} and each of these carriers has individual storage capacities. Within a constraint, storage capacities for a carrier c are compared with dispatch variables of all the carriers $\hat{c}$ explicitly stored. The corresponding constraints are given by Eqs. 26a to 26c.

$$s(t) \sum_{\hat{c} \in \delta^{+}_{c} \cap \gamma^{st}_{e}} \sum_{\langle \hat{t},\hat{r}\rangle \in \sigma_{t,r,\hat{c}}} \sum_{m \in \mu_{e}} \frac{St^{in}_{\hat{t},\tilde{t},\hat{r},\hat{c},e,m}}{ava^{stI}_{\hat{t},\tilde{t},\hat{r},\hat{c},e,m}} \leq \sum_{\hat{r} \in \eta^{sp}_{e} \cap \delta^{+}_{r}} Cap^{opr,stI}_{\alpha^{sup}_{t},\tilde{t},\hat{r},e,c} \quad \forall e \in \Gamma^{st}_{e},\ c \in \gamma^{stCap}_{e},\ \langle t,r\rangle \in \varphi_{c},\ \tilde{t} \in \theta^{dis}_{e,t} \tag{26a}$$

$$s(t) \sum_{\hat{c} \in \delta^{+}_{c} \cap \gamma^{st}_{e}} \sum_{\langle \hat{t},\hat{r}\rangle \in \sigma_{t,r,\hat{c}}} \sum_{m \in \mu_{e}} \frac{St^{out}_{\hat{t},\tilde{t},\hat{r},\hat{c},e,m}}{ava^{stO}_{\hat{t},\tilde{t},\hat{r},\hat{c},e,m}} \leq \sum_{\hat{r} \in \eta^{sp}_{e} \cap \delta^{+}_{r}} Cap^{opr,stO}_{\alpha^{sup}_{t},\tilde{t},\hat{r},e,c} \quad \forall e \in \Gamma^{st}_{e},\ c \in \gamma^{stCap}_{e},\ \langle t,r\rangle \in \varphi_{c},\ \tilde{t} \in \theta^{dis}_{e,t} \tag{26b}$$

$$\sum_{\hat{c}\in\delta_c^+\cap\gamma_e^{st}} \sum_{\langle\hat{t},\hat{r}\rangle\in\sigma_{t,r,\hat{c}}} \sum_{m\in\mu_e} \frac{stLvl_{\hat{t},\tilde{t},\hat{r},\hat{c},e,m}}{ava^{stL}_{\hat{t},\tilde{t},\hat{r},\hat{c},e,m}} \leq \sum_{\hat{r}\in\eta_e^{sp}\cap\delta_r^+} Cap^{opr,stS}_{\alpha_t^{sup},\tilde{t},\hat{r},e,c} \qquad \forall e \in \Gamma_e^{st},\, c \in \gamma_e^{stCap},\, \langle t,r\rangle \in \varphi_c,\, \tilde{t} \in \theta^{dis}_{e,t} \tag{26c}$$

Unlike all other capacities, constraints on storage size do not include a scaling factor, because storage size already is provided in energy units.

For exchange, similar to storage, capacities are created for all regions and carriers defined in $\beta_{c,r}$ and capacities are then compared with dispatch variables $\hat{c}$ explicitly exchanged. Exchange capacities can be directed, meaning the energy transportable from r to r' and from r' to r can differ.

$$s(t) \sum_{\hat{c}\in\lambda(c)} \sum_{\langle\hat{t},\hat{r}\rangle\in\sigma_{t,r,\hat{c}}} \sum_{\hat{r}'\in\rho_{\hat{c}}\cap\delta^+_{r'}} Exc_{\hat{t},\hat{r},\hat{r}',c} \leq Cap^{opr,exc}_{\alpha_t^{sup},r,r',c} \qquad \forall\langle c,\, r\rangle \in \{V(C) \times V(R) \,|\, \beta_{c,r}\},\, r' \in \beta_{c,r},\, t \in \tau_c \tag{27}$$

Lastly, trade variables are subject to capacity constraints. Unlike conversion, storage and exchange, capacities for trade are not a variable but an exogenous parameter. In Eq. 28 the corresponding constraint for all bought quantities is provided.

$$s(t)\, Trd^{buy}_{t,r,c,i} \leq cap^{buy}_{t,r,c,i} \qquad \forall c \in V(C),\, \langle t,r\rangle \in \varphi_c,\, i \in \zeta^{buy} \tag{28}$$

3.6. Expansion

The operated capacities $Capa^{opr}$ for conversion, storage and exchange that restrict dispatch variables do not necessarily match installed capacities $Capa^{ist}$. The framework can endogenously decide to decommission installed capacities before the end of their technical lifetime to mitigate operating costs. The following constraints achieve this for conversion capacities and are equally applicable for storage and exchange:

$$Cap^{opr,cv}_{t,\tilde{t},r,e} \leq Cap^{ist,cv}_{t,\tilde{t},r,e} \qquad \forall e \in \Gamma^{cv}, t \in \Phi, \tilde{t} \in \theta^{dis}_{e,t}, r \in \eta_e^{sp} \tag{29}$$

$$Cap^{opr,cv}_{t,\tilde{t},r,e} \leq Cap^{opr,cv}_{t-1,\tilde{t},r,e} + Exp^{cv}_{t,r,e} \qquad \forall e \in \Gamma^{cv}, t \in \Phi, \tilde{t} \in \theta^{dis}_{e,t}, r \in \eta_e^{sp} \tag{30}$$

Eq. 29 simply ensures operated capacities do not exceed installed capacities. To avoid that decommissioned capacities are put into operation again, Eq. 30 demands that any rise in operated capacity has to result from capacity expansion, which is denoted as $Exp^{cv}_{t,r,c,e}$.

Installed capacities are a result of pre-existing capacities and capacity expansion. Analogously to expansion regions, time-steps of expansion are termed η_e^{tp} and their resolution corresponds to the most detailed resolution across all carriers assigned as well:

$$\eta_e^{tp} = \{V(R) \,|\, d(r) = \max_{c\in\gamma_e^{in}\cup\gamma_e^{out}} (dep_c^{exp,tp})\} \tag{31}$$

As explained in section 2.4, certain technologies are differentiated by time-step of construction, for others the time-step of construction is irrelevant and yet others cannot be expanded at all. This affects how expansion variables have to be aggregated to obtain installed capacities and is reflected by the set $\theta^{exp}_{e,\tilde{t},t}$ defined in Eq. 32. The set provides all expansion time-steps to be aggregated for obtaining capacities of technology e with construction period $\tilde{t}$ at time-step t. Consequently, this set is empty for technologies that cannot be expended. For *mature* technologies it contains all time-steps of expansion that result in a life-span including t. For *emerging* technologies, capacities build in different years are not aggregated and accordingly only $\tilde{t}$ itself is assigned.

$$\theta^{exp}_{e,t,\tilde{t}} = \begin{cases} \emptyset & \text{,if } g(e) = \text{‘}stock\text{’} \\ \{\tilde{t}' \in \eta_e^{tp} \,|\, \tilde{t}' \in (\alpha_t^{sup} - lt^{tech}_{e,\tilde{t}'}, \alpha_t^{sup}]\} & \text{,if } g(e) = \text{‘}mature\text{’} \\ \{\tilde{t}\} & \text{,if } g(e) = \text{‘}emerging\text{’} \end{cases} \tag{32}$$

Building on this, in 33 the installed capacities are defined as the sum of the expansion plus any pre-existing capacities $capa^{pre}$ that refer to pre-existing capacities set exogenously.

$$Cap^{ist,cv}_{t,\tilde{t},r,e} = cap^{pre,cv}_{t,\tilde{t},r,e} + \sum_{\tilde{t}'\in\theta^{exp}_{e,\tilde{t},t}} Exp^{cv}_{\tilde{t}',r,e} \qquad \forall e \in \Gamma^{cv}, t \in \Phi, \tilde{t} \in \theta^{dis}_{e,t}, r \in \eta_e^{sp} \tag{33}$$

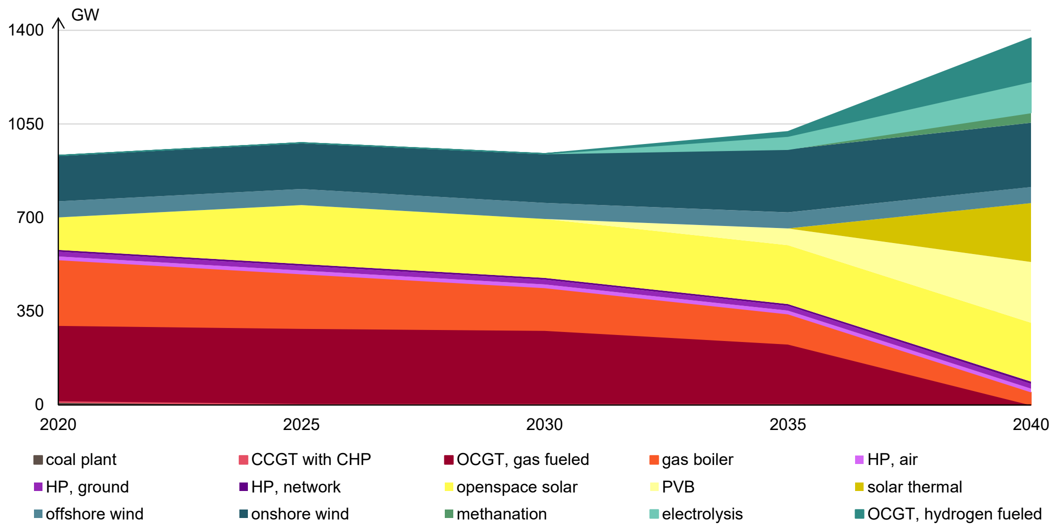

Figure 7: Operated conversion capacities for the example model

4. Solving the example model

To demonstrate feasibility of the framework's approach, the model its introduction was based on is now created and solved. A particular focus is on how temporal granularity impacts model size, solve time and final results.

4.1. Results of the example model

The example model was parameterized as follows: For location-dependent parameters, like demand or availability of renewables, values were selected such that the regions *East* and *West* resemble Germany and France, but detailed pre-existing capacities were not provided. Costs and technological properties were based on recent estimates. To actually achieve the high levels of renewables and sector integration the framework was developed for, the yearly emission limit linearly decreases from 350 million tons in 2020 to zero in 2040.

The development of operated conversion capacities that results from these parameters when solving the model is displayed in Fig. 7. It should be noted that according to the framework's convention, these are input capacities. So, in case of heatpumps (HP) for example, potential heat output exceeds the represented value that refers to electricity input. In the graph, the impact of moving from a small emissions limit in 2035 to no emissions in 2040 is very pronounced. Instead of switching to synthetic gas, gas boilers and OCGT power plants are mostly decommissioned and replaced with solar heating and hydrogen turbines. The resulting energy flow for 2040 is shown in Fig. 8, which is the quantitative counterpart to Fig. 5 from section 2.4. Again, colored vertices represent energy carriers and grey vertices correspond to technologies. The graph visualizes several characteristics of the framework's graph-based approach. For example, the flow leaving *district heat* and entering *heat* reflects that according to the energy balance in Eq. 13, descendant carriers are included in an ancestors energy balance. As a result, *district heat* can equally satisfy final demand for *heat* despite being produced by different technologies. Also, both *hydrogen* and *synthetic gas* flows enter and leave the *gas storage* technology, which was defined to store their ancestor *gas*. This corresponds to the storage implementation presented in sections 2.4 and 3.3.

4.2. Impact of temporal resolution

All these results were obtained solving the model with full foresight and the settings outlined in section 2.3, which proposed an hourly resolution for electricity, four-hour steps for heat and daily balancing of all gaseous carriers. To study the impact of impact temporal granularity, two more detailed scenarios are considered in addition. One extends hourly granularity to *heat* and *district heat*, while all other resolutions remain unchanged. In the other, all carriers are modelled hourly.

In Fig. 9 the size and number of non-zero elements for the model's underlying optimization matrix are shown across all three scenarios. Even though three-quarters of technologies in the model either use or generate electricity, reducing temporal granularity for all carriers but electricity achieves a reduction of about 50% in matrix size and number of

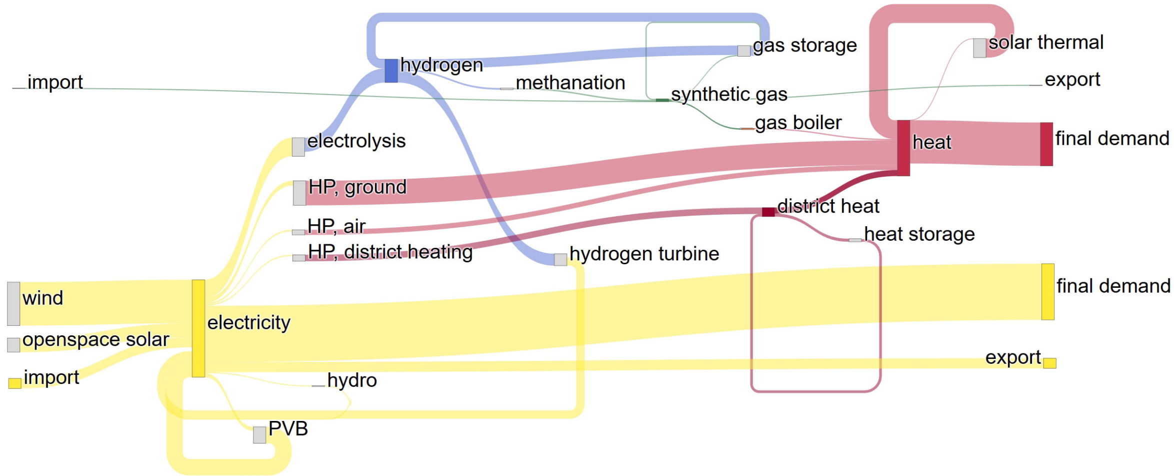

Figure 8: Quantitative energy flow in example model for the year 2040

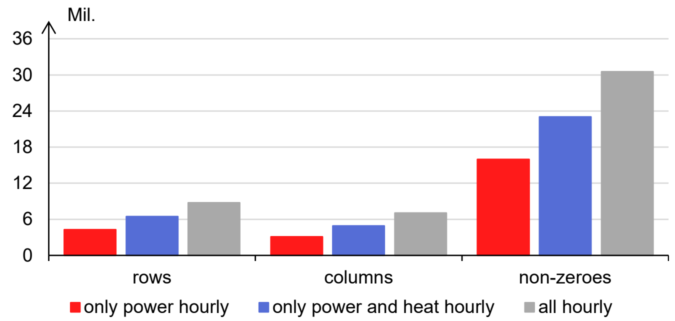

Figure 9: Model size across scenarios

non-zero elements. If resolution for heat and electricity is kept hourly and detail is only decreased for gaseous carriers, the reduction still amounts to 25%. A reduced model size will decrease working memory requirements and allow to solve models that previously did not fit into memory, but it does not necessarily reduce computation time. The time to solve a problem also depends on the inner structure of the matrix and the applied solution algorithm.

To assess the scenarios in terms of computation time, they were solved using different algorithms of the Gurobi solver. Using the simplex method did not provide any results in less than a day; solve times when applying the Barrier algorithm with 'Approximate Minimum Degree' or 'Nested Dissection' ordering are displayed in Fig. 10.[6] Results indicate that the reduction in solve time is actually disproportionately high to model size. When going from an hourly granularity for all carriers to only modelling electricity hourly, model size was reduced by 50%, but solve time decreased by 64% to 75% depending on the ordering method. The corresponding computations were run on a high-performance computing (HPC) cluster. If reproduced on a desktop computer with less working memory and parallel processors, the model creation might take longer, because the framework heavily utilizes multi-threading. Also, for 'Nested Dissection' ordering, memory limits are likely to be exceeded.

Lastly, final model results are compared for the three scenarios. To this end, Fig. 11 shows the difference in operated capacities for the two more detailed scenarios compared to the reference case for 2040. Positive values indicate that capacities for the more detailed scenario exceed results from the reference case. Only technologies where results differ areincluded. If heat is modelled hourly, generation from CHP plants and solar heating is partly replaced by more flexible gas boilers fueled by synthetic gas. To generate this gas, additional capacities for electrolysis and methanation are required. CHP plants generating less leads to smaller seized heat storage. Also, reduced solar thermal capacities

[6]Reported times only refer to the barrier algorithm itself and omit crossover. In no case crossover improved results by more than 7×10^{-6} percent, but typically increased computation time by a factor of four.

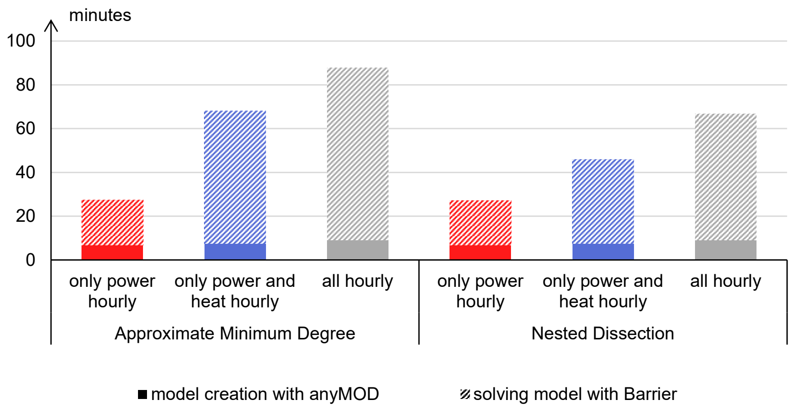

Figure 10: Solve time with Barrier algorithm across scenarios

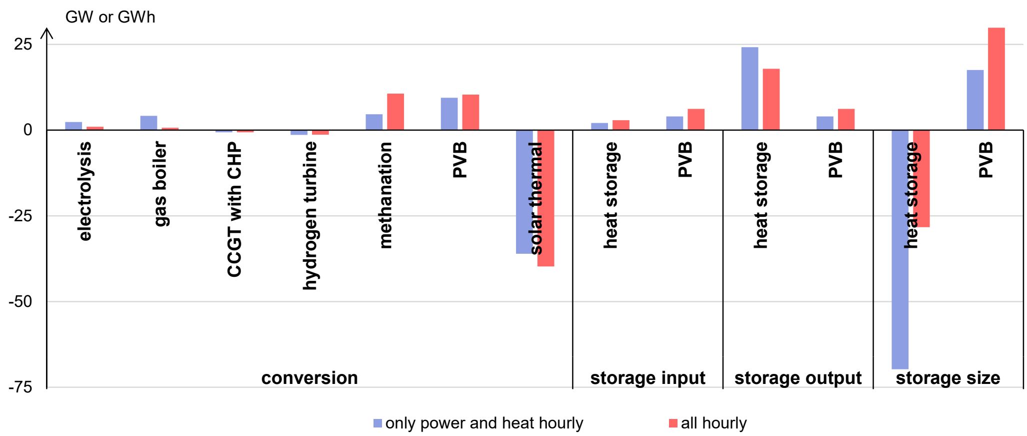

Figure 11: Operated capacities compared to reference case in 2040

allow to install additional PVB systems, since both technologies compete for rooftop area. If the resolution of gas is changed from daily to hourly as well, shifting gas within the day requires gas storage and thus becomes subject to losses. Consequently storing gas is avoided and instead methanation capacities are increased to produce gas when its demanded. For the reference case system costs amount to 397.4 billion and increase to 399.6 billion when heat is additionally modelled at an hourly resolution. Modelling all carriers hourly further increases costs to 400.1 billion.

Deviations between the reference case and more detailed scenarios should not necessarily be interpreted as inaccuracies. If a less detailed resolution can be justified from an engineering perspective, it does not only reduce model size, but also allows to account for a system's inherent flexibility. Consequently, the decrease in system costs when reducing a carrier's granularity can be interpreted as the economic value of this flexibility. The effects that changing the granularity of a single carrier has across the entire system also emphasizes what was stated at the very beginning of the introduction: Analysing energy systems characterized by high shares of intermittent renewables requires a cross-sectoral perspective.

5. Conclusion and outlook

This paper introduced an open framework for energy system modelling with multiple periods of capacity expansion. In contrast to existing tools, the frameworks pursues a novel approach based on graph theory. Organizing sets in rooted trees enables two features that facilitate modelling systems with high shares of renewables and sector integration. As a result, model size can be reduced without reducing the level of detail applied to fluctuating renewables. In addition, flexibility inherent to the system, for example in the gas network, can be accounted for. Second, substitution of energy carriers can be modelled in dependance of the respective context: conversion, storage, transport, or demand. This achieves a more comprehensive representation of how technologies and energy carriers can interact in an integrated energy system. In addition, smaller features not found in previous frameworks, namely an accurate representation of technological advancement, endogenous decommissioning and internal storage of generated carriers, have been implemented.

So far, the framework cannot account for weather related uncertainties of renewable generation, although this has been identified as a key requirement for modelling high shares of renewables [37]. Therefore, the focus of further development is to enable stochastic capacity expansion to account for a range of weather years. Since this implies a substantial increase in model size, a particular challenge lies in solving such models. One approach could be to implement a distributed solution algorithm based on Benders decomposition that can fully exploit the capabilities of HPC [9]. For this purpose the original model should be decomposed into a small master problem, which addresses capacity expansion, and several large subproblems addressing dispatch. These subproblems could then be solved simultaneously to reduce computation time.

Other potential improvements include the implementation of must-run constraints, ramping constraints and a representation of demand-side management based on existing approaches [43, 13].

6. Acknowledgements

The research leading to these results has received funding from the European Union's Horizon 2020 research and innovation programme under grant agreement No 773406.

References

[1] Bataille, C., Åhman, M., Neuhoff, K., Nilsson, L., Fischedick, M., Lechtenböhmer, S., Solano-Rodriquez, B., Denis-Ryan, A., Stiebert, S., Waisman, H., Sartor, O., Rahbar, S., 2018. A review of technology and policy deep decarbonization pathway options for making energy-intensive industry production consistent with the paris agreement. Journal of Cleaner Production 187, 960–973. doi:10.1016/j.jclepro.2018.03.107.

[2] Bauknecht, D., Funcke, S., Vogel, M., 2020. Is small beautiful? a framework for assessing decentralised electricity systems. Renewable and Sustainable Energy Reviews 118, 109543. doi:10.1016/j.rser.2019.109543.

[3] Bezanson, J., Edelman, A., Karpinski, S., Shah, V., 2017. Julia: A fresh approach to numerical computing. SIAM Review 59(1), 65–98. doi:10.1137/141000671.

[4] Bloess, A., 2019. Impacts of heat sector transformation on germany's power system through increased use of power-to-heat. Applied Energy 239, 560–580. doi:10.1016/j.apenergy.2019.01.101.

[5] Bondy, J., Murty, U., 2008. Graph Theory. Springer.

[6] Brown, T., Bischof-Niemz, T., Blok, K., Breyer, C., Lund, H., Mathiesen, B., 2018a. Response to 'burden of proof: A comprehensive review of the feasibility of 100% renewable-electricity systems'. Renewable and Sustainable Energy Reviews 92, 834–847. doi:10.1016/j.rser.2018.04.113.

[7] Brown, T., Schlachtberger, D., Kies, A., Schramm, S., Greiner, M., 2018b. Synergies of sector coupling and transmission extension in a cost-optimised, highly renewable european energy system. Renewable and Sustainable Energy Reviews 160, 720–739. doi:10.1016/j.energy.2018.06.222.

[8] Burre, J., Bongartz, D., Brée, L., Roh, K., Mitsos, A., 2020. Power-to-x: Between electricity storage, e-production, and demand side management. Chemie Ingenieur Technik 92, 74–84. doi:10.1002/cite.201900102.

[9] Conejo, A., Castillo, E., Minguez, R., Garcia-Bertrand, R., 2006. Decomposition Techniques in Mathematical Programming. Springer.

[10] Diestel, R., 2000. Graph Theory. Springer.

[11] Doucette, R., McCulloch, M., 2011. Modeling the co2 emissions from battery electric vehicles given the power generation mixes of different countries. Energy Policy 39, 803–811. doi:10.1016/j.enpol.2010.10.054.

[12] Gardumi, F., Shivakumar, A., Morrison, R., Taliotis, C., Broad, O., Beltramo, A., Sridharan, V., Howells, M., Hörsch, J., Niet, T., Almulla, Y., Ramos, E., Burandt, T., Balderrama, G., Pinto de Moura, G., Zepeda, E., Alfstad, T.a., 2018. From the development of an open-source energy modelling tool to its application and the creation of communities of practice: The example of osemosys. Energy Strategy Reviews 20, 209–228. doi:10.1016/j.esr.2018.03.005.

[13] Gerbaulet, C., Casimir, L., 2017. dynelmod: A dynamic investment and dispatch model for the future european electricity market. DIW Data Documentation URL: http://hdl.handle.net/10419/161634.

[14] Gerbaulet, C., Hirschhausen, C., Kemfert, C., Lorenz, C., Oei, P., 2019. European electricity sector decarbonization under different levels of foresight. Renewable Energy 141, 973–987. doi:10.1016/j.renene.2019.02.099.

[15] Groissböck, M., 2019. Are open source energy system optimization tools mature enough for serious use? Renewable and Sustainable Energy Reviews 102, 234–248. doi:10.1016/j.rser.2018.11.020.

[16] Hauser, P., . A modelling approach for the german gas grid using highly resolved spatial, temporal and sectoral data (gamamod-de). EconStor Preprints URL: https://ideas.repec.org/p/zbw/esprep/197000.html.

[17] Haydt, G., Leal, V., Pina, A., Silva, C., 2011. The relevance of the energy resource dynamics in the mid/long-term energy planning models. Renewable Energy 36, 3068–3074. doi:10.1016/j.renene.2011.03.028.

[18] Heggarty, T., Bourmaud, J.Y., Girard, R., Kariniotakis, G., 2019. Multi-temporal assessment of power system flexibility requirement. Applied Energy 238, 1327–1336. doi:10.1016/j.apenergy.2019.01.198.

[19] Howells, M., Rogner, H., Strachan, N., Heaps, C., Huntington, H., Kypreos, S., Hughes, A., Silveira, S., DeCarolis, J., Bazillian, M., Roehrl, A.a., 2011. Osemosys: The open source energy modeling system: An introduction to its ethos, structure and development. Energy Policy 39(10), 5850–5870. doi:10.1016/j.enpol.2011.06.033.

[20] Kondziella, H., Bruckner, T., 2016. Flexibility requirements of renewable energy based electricity systems – a review of research results and methodologies. Renewable and Sustainable Energy Reviews 53, 10–22. doi:10.1016/j.rser.2015.07.199.

[21] Kotzur, L., Markewitz, P., Robinius, M., Stolten, D., 2018. Time series aggregation for energy system design modeling seasonal storage. Applied Energy 213, 123–135. doi:10.1016/j.apenergy.2018.01.023.

[22] Lopion, P., Markewitz, P., Robinius, M., Stolten, D., 2018. A review of current challenges and trends in energy systems modeling. Renewable and Sustainable Energy Reviews 96, 156–166. doi:10.1016/j.rser.2018.07.045.

[23] Lund, P., Lindgren, J., Mikkola, J., Salpakari, J., 2015. Review of energy system flexibility measures to enable high levels of variable renewable electricity. Renewable and Sustainable Energy Reviews 45, 785–807. doi:10.1016/j.rser.2015.01.057.

[24] Löffler, K., Burandt, T., Hainsch, K., Oei, P., 2019. Modeling the low-carbon transition of the european energy system - a quantitative assessment of the stranded assets problem. Energy Strategy Reviews 26, 100422. doi:10.1016/j.esr.2019.100422.

[25] Nahmacher, P., Schmid, E., Hirth, L., Knopf, B., 2016. Carpe diem: A novel approach to select representative days for longterm power system modeling. Energy 112, 430–442. doi:10.1016/j.energy.2016.06.081.

[26] Oberle, S., Elsland, R., 2019. Are open access models able to assess today's energy scenarios? Energy Strategy Reviews 26, 100396. doi:10.1016/j.esr.2019.100396.

[27] Open Knowledge Foundation, 2020. Open definition. URL: https://opendefinition.org/od/2.1/en/.

[28] Orths, A., Anderson, C., Brown, T., Mulhern, J., Pudjianto, D., Ernst, B., O'Malley, M., McCalley, J., Strbac, G., 2019. Flexibility from energy systems integration: Supporting synergies among sectors. IEEE Power and Energy Magazine 17(6), 67–87. doi:10.1109/MPE.2019.2931054.

[29] Petrovic, B., Rogers, H., Hecking, H., Schulte, S., Weiser, F., 2017. Future european gas transmission bottlenecks in differing supply and demand scenarios. Oxford Institute for Energy Studies 119. URL: https://ora.ox.ac.uk/objects/uuid:9486b8a3-2c4c-4991-a4ef-c4cd27cf928f.

[30] Pfenniger, S., 2017. Energy scientists must show their workings. Nature 542(7642), 393–393. doi:10.1038/542393a.

[31] Pfenniger, S., DeCarolis, J., Hirth, L., Quoilin, S., Staffel, I., 2017. The importance of open data and software: Is energy research lagging behind? Energy Policy 101, 211–215. doi:10.1016/j.enpol.2016.11.046.

[32] Pfenniger, S., Pickering, B., 2018. Calliope: a multi-scale energy systems modelling. The Journal of Open Source Software 3(29), 825. doi:10.21105/joss.00825.

[33] Pfenninger, S., Hawkes, A., Keirstead, J., 2014. Energy systems modeling for twenty-first century energy challenges. Renewable and Sustainable Energy Reviews 33, 74–86. doi:10.1016/j.rser.2014.02.003.

[34] Pfenninger, S., Pickering, B., Tröndle, T., Garchery, M., Hawker, G., Lombardi, F., 2020. Calliope documentation release 0.6.5. URL: https://readthedocs.org/projects/calliope/.

[35] Poncelet, K., Delarue, E., Six, D., Duerinck, J., D'haeseleer, W., 2016. Impact of the level of temporal and operational detail in energy-system planning models. Applied Energy 162, 631–643. doi:10.1016/j.apenergy.2015.10.100.

[36] Renaldi, R., Friedrich, D., 2017. Multiple time grids in operational optimisation of energy systems with short- and long-term thermal energy storage. Energy 133, 784–795. doi:10.1016/j.energy.2017.05.120.

[37] Ringkjøb, H., Haugan, P., Solbrekke, I., 2018. A review of modelling tools for energy and electricity systems with large shares of variable renewables. Renewable and Sustainable Energy Reviews 96, 440–459. doi:10.1016/j.rser.2018.08.002.

[38] Schopfer, S., Tiefenbeck, V., Staake, T., 2018. Economic assessment of photovoltaic battery systems based on household load profiles. Applied Energy 223, 229–248. doi:10.1016/j.apenergy.2018.03.185.

[39] Thellufsen, J., Lund, H., 2017. Cross-border versus cross-sector interconnectivity in renewable energy systems. Energy 124, 492–501. doi:10.1016/j.energy.2017.02.112.

[40] Weibezahn, J., Kendziorski, M., 2019. Joulia.jl – a large-scale spatial open-source electricity sector model using the julia language. Energies 12, 1153. doi:10.5281/zenodo.1044463.

[41] Welsch, M., Howells, M., Bazilian, M., DeCarolis, J., Hermann, S., Rogner, H., 2012. Modelling elements of smart grids e enhancing the osemosys (open sourceenergy modelling system) code. Energy 46, 337–350. doi:10.1016/j.energy.2012.08.017.

[42] Wiese, F., Hilpert, S., Kaldemeyer, C., Pleßmann, G., 2018. A qualitative evaluation approach for energy system modelling frameworks. Energy, Sustainability and Society 8, 13. doi:10.1186/s13705-018-0154-3.

[43] Zerrahn, A., Schill, W.P., 2015. On the representation of demand-side management in power system models. Energy 84, 840–845. doi:10.1016/j.energy.2015.03.037.